State-to-state oxygen kinetics behind reflected shock waves: Assessment of different approaches FREE

D. Kravchenko ✉; O. Kunova; E. Kustova; M. Melnik

Check for updates

View Online   Export Citation   CrossMark

State-to-State Oxygen Kinetics behind Reflected Shock Waves: Assessment of Different Approaches

D. Kravchenko,[1, 2, a)] O. Kunova,[1, 2, b)] E. Kustova,[1, 2, c)] and M. Melnik[1, 2, d)]

[1)]*Saint Petersburg State University, 7/9 Universitetskaya nab., St. Petersburg, 199034, Russian Federation.*
[2)]*Federal Research Center "Computer Science and Control" of the Russian Academy of Sciences, 44/2 Vavilova ul., Moscow, 119333, Russian Federation.*

[a)]*Corresponding author: kravchenk06.denis@gmail.com*
[b)]*Electronic mail: o.kunova@spbu.ru*
[c)]*Electronic mail: e.kustova@spbu.ru*
[d)]*Electronic mail: melnik.mxm@gmail.com*

Abstract. We study the influence of vibrational and chemical relaxation behind the incident shock wave on the gas parameters behind the reflected wave. The detailed state-to-state approach is used to simulate the shock tube experiment for the pure oxygen flow. We extend our previous work including comparison with experimentally measured pressure time-histories behind the reflected shock wave. The vibrational temperature time-histories are compared with both experimental and theoretical data obtained recently using simulations based on quasiclassical trajectory (QCT) method. The results show a weak role of dissociation reactions and, on the contrary, a significant effect of vibrational relaxation in the region between the incident and reflected shock waves on the pressure and temperature profiles. The best agreement with the experimental vibrational temperature is obtained for the combination of the Schwartz–Slawsky–Herzfeld (SSH) model of vibrational energy transitions and the state-specific Marrone–Treanor dissociation model with the parameter $U = 3T$. Three different definitions of the vibrational temperature are assessed, and their equivalence is proved. For more accurate comparison with experimental data we propose an additional correction to the experimental error which takes into account the effect of vibrational relaxation between the incident and reflected shocks. This correction is found large near the reflected shock front but tends to zero with rising distance.

09 February 2024 10:23:15

INTRODUCTION

For a wide range of flow conditions, taking into account non-equilibrium between the internal and translational degrees of freedom is significant. Strong deviations from thermal and chemical equilibrium are observed in electric and microwave discharges, laser systems, microchannels and especially behind shock waves (SWs) near descent vehicles. Under such conditions, chemical reactions and vibrational relaxation of the gas are strongly coupled and affect the flow macroparameters. For accurate modeling that kind of high-enthalpy flows, it becomes necessary to use detailed models of non-equilibrium vibrational-chemical kinetics.

Whereas for sufficiently rarefied gases direct Monte-Carlo simulations (DSMC) [1, 2] provide the best results, for more dense gases this method becomes computationally expensive. Therefore, development and assessment of continuum approaches capable to capture non-equilibrium effects is a relevant task. Among continuum models, one of the most detailed is the state-to-state approach based on the fluid-dynamic equations coupled with the balance equations for populations of each molecular vibrational level [3]. This approach also requires considerable computational costs (although much less then DSMC), and thus its validation on simple problems is required. The most common test cases used for the model assessment are: spatially homogeneous isothermal or adiabatic bath relaxation [4, 5] and one-dimensional steady flows behind a shock wave [2, 6, 7, 8, 9, 10]. During the last decade, shock tube experiment [11] on oxygen vibrational-chemical kinetics behind an incident SW was the main benchmark for such conditions. However, multiple attempts to simulate this experiment encountered difficulties [7, 10, 12]. Recent experiments on oxygen relaxation behind reflected shock waves [13] provide an excellent opportunity for validating different kinetic approaches in a wider temperature range using the data on vibrational temperature, absorbance and pressure. This opportunity has already been used in [14] for the method based on quasi-classical trajectory (QCT) simulations and in [15] for the state-to-state approach developed by the authors of the present work. In both studies, a significant effect of vibrational relaxation between incident and reflected shock waves on the vibrational temperature and pressure was found, and a question about correct interpretation of experimental results was raised.

This study aims at further comparison of state-to-state simulations behind reflected SW with the results obtained experimentally [13] as well as with simulations of [14]. In addition to previous results we 1) analyze calculated pressure time-histories compared to the experimental ones; 2) discuss the effect of various definitions of vibrational temperature; 3) compare the vibrational temperature and the degree of dissociation between the incident and reflected SWs with those reported in [14].

THEORETICAL MODEL

Detailed description of the theoretical model and methodology can be found in [15]. Here we briefly remind the main set of equations based on the zero-order approximation of the Chapman–Enskog method in the state-to-state formulation [3]. Governing equations for a one-dimensional stationary flow of O_2/O mixture include balance equations for the population of the i-th vibrational state of molecules n_i and number densities of atoms n_a:

$$v\frac{dn_i}{dx} + n_i\frac{dv}{dx} = R_i^{vibr} + R_i^{react}, \quad i = 0,\ 1,\ \dots\ l, \tag{1}$$

$$v\frac{dn_a}{dx} + n_a\frac{dv}{dx} = -2\sum_i R_i^{react} \tag{2}$$

and the equations of mass, momentum and energy conservation:

$$\rho v = \text{const}, \tag{3}$$

$$\rho v^2 + p = \text{const}, \tag{4}$$

$$\frac{E+p}{\rho} + \frac{v^2}{2} = \text{const}. \tag{5}$$

Here v is the gas velocity, R_i^{vibr} and R_i^{react} are relaxation terms describing the change in the populations due to the vibrational energy exchange and chemical reactions, l is the maximum vibrational level of the molecule, ρ and p are the density and pressure of the gas, and E is the total energy per unit volume.

The kinetic scheme includes transitions of translational energy into vibrational and vice versa (VT-exchanges); vibrational energy exchanges in the collisions of molecules (VV-exchanges); the dissociation reaction and the backward recombination reaction in a collision with a molecule or an atom. The vibrational energy exchanges were described using the generalized Schwartz–Slawsky–Herzfeld theory (SSH theory) [16] and the forced harmonic oscillator (FHO) model [17]. The vibrational energy was calculated using the anharmonic oscillator model. The dissociation processes were described using the Marrone–Treanor (MT) model [18] with the Arrhenius law parameters from [19] and the most common parameter U values found in the literature: $U = D/6k$, $3T$, and ∞, as well as the parameters proposed in [20]. Here D is the dissociation energy of molecules, k is the Boltzmann constant, and T is the gas translational-rotational temperature.

The peculiarity of our approach is that we take into account vibrational and chemical kinetics in a flow between the incident and reflected SWs. For modelling an incident SW, the algorithm is quite simple: first, the gas parameters just behind the front are calculated on the basis of conservation laws using the assumption of frozen vibrational-chemical kinetics; then system (1)–(5) is integrated numerically until the equilibrium is attained. The reflected SW problem is more complicated not only because of double recalculations of the gas parameters after the shock fronts, but also due to the non-equilibrium of the gas between the two SWs. Note that in order to reproduce theoretically experimental measurements, the authors of experiment [13] apply the assumption of frozen chemistry and vibrational relaxation after an incident SW. This assumption is justified by the low pressure and a short time until reflected SW appears. However, studies [14] and [15] demonstrated significant discrepancies in the gas parameters caused by partial relaxation between the shocks. Moreover, it was shown that the time between the passage of the incident and reflected SWs is comparable with the measurement times. In the present study, we assume that the reflected SW propagates through the non-equilibrium gas. Eqs. (1)–(5) are first solved in the time range between the incident and reflected SWs passage, and this solution is taken as initial conditions for the reflected shock problem. Using this technique, we assess different models of vibrational-chemical coupling by comparison with experiments and simulations of [14].

RESULTS AND DISCUSSION

Numerical simulation of stiff ordinary differential equations (1)–(5) was carried out by the Runge–Kutta method with variable step size (ode15s, MATLAB); for more details see [15]. Kinetics of pure oxygen under experimental conditions from [13] is considered; two test cases are discussed, see Table I for the initial conditions.

We start our analysis discussing the pressure, which is the most reliable parameter since it is measured directly in the experiment and not calculated by subsequent data processing. Preliminary assessment of the pressure values was carried out in [15], but only by comparing the values at the moment of the reflected SW appearance. That is due to the

TABLE I. Experimental conditions for test cases 1 and 6 of [13]. p_{fill} is the initial pressure in the tube; p^0 and T_{tr}^0 are the pressure and temperature immediately behind the front of the reflected SW, respectively; U_{is} and U_{rs} are the velocities of the incident and reflected SWs, respectively.

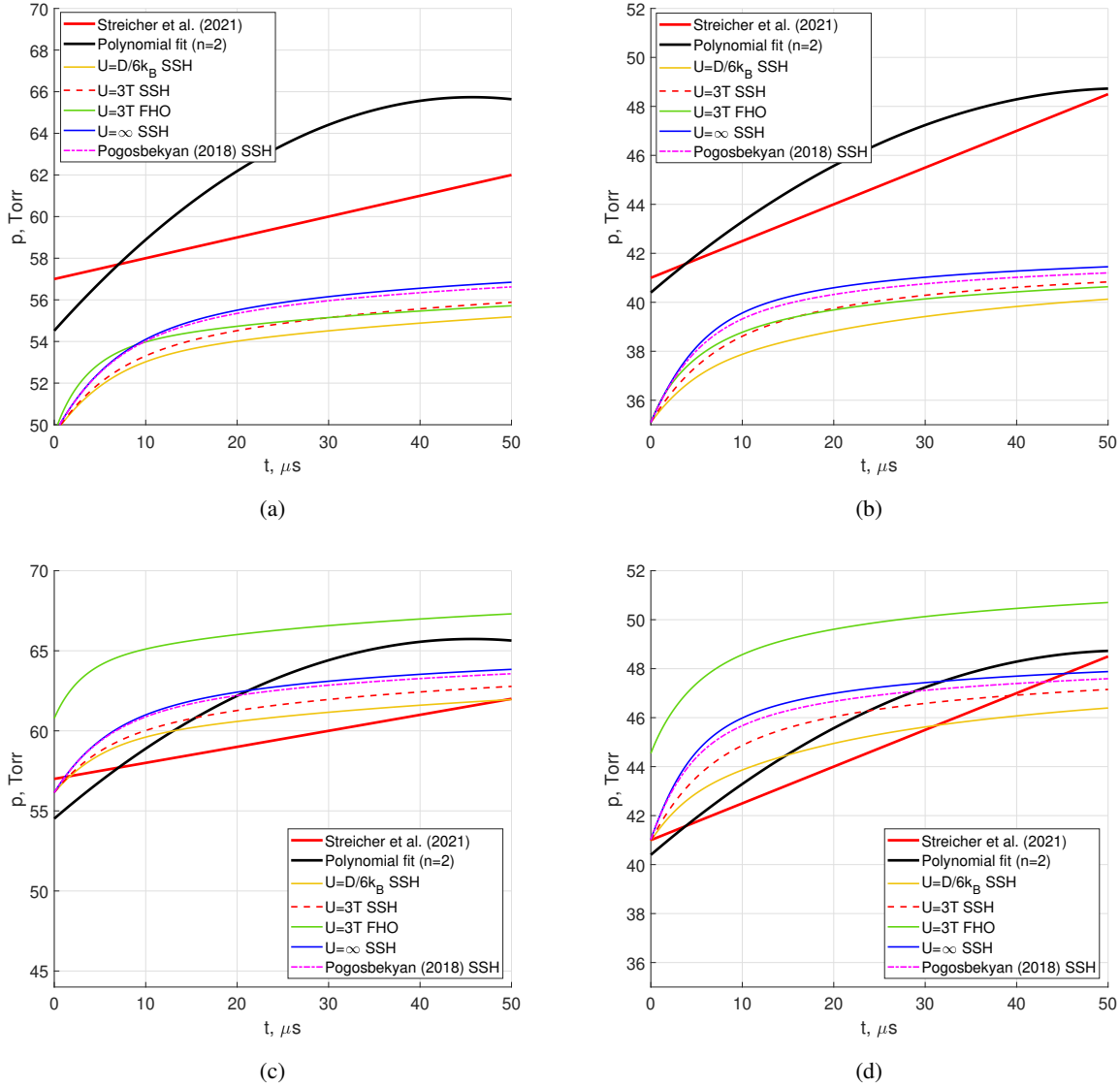| No.	p_{fill}, Torr	p^0, Torr	T_{tr}^0, K	U_{is}, m/s	U_{rs}, m/s
1	0.13	57	6230	2220	770
6	0.07	41	7940	2510	870

FIGURE 1. Pressure time-histories behind the front of the reflected SW for initial conditions no. 1 (a, c) and no. 6 (b, d) taking into account relaxation after the incident shock wave (c, d) and without it (a, b).

absence of the pressure time-histories in [13] for pure oxygen test cases. For the present study, the data were received from the authors of [13] in a private communication.

The time characteristics of the pressure are presented in Fig. 1. The authors of experiment used a linear approximation of the raw pressure data. For more accurate comparison, we present here the least-squares polynomial fit of

the raw data. The degree of polynomial fit is $n = 2$, however, almost the same curve was obtained with $n = 3$. This fit provides a much better description of the measurements for the first 50 μs than the linear approximation. The raw data is not plotted here since it is not published by the authors of [13].

It can be seen from Fig. 1 that neglecting partial relaxation between the incident and reflected shock waves yields poor predictions for both the initial pressure values and the general trend of the pressure evolution. Since before the reflected SW all vibrational energy exchanges are frozen in this case, there is no difference in the initial values for the FHO and SSH models. Contrarily, in the case when partial relaxation is taken into account, the simulated pressure distributions are much closer to the measured pressure time-histories. Both the general trend and pressure initial values immediately behind the reflected SW are predicted rather well. The best accuracy is obtained using the SSH theory in combination with the Marrone–Treanor dissociation model with the parameter $U = 3T$. The FHO model in this case overestimates initial pressure values. A possible reason for this pressure overprediction is the use of a simplified FHO model that does not account for the three-dimensional nature of molecule rotations during a collision. This hypothesis will be assessed in future studies using the FHO-FR (free-rotating) model [21, 22]. Summarizing the results on the pressure distributions, we confirm once again our previous conclusion [15] about the importance of the vibrational relaxation between SWs.

Let us estimate now the role of chemical reactions between the SWs. Figure 2 shows the mole fraction of atomic oxygen χ_O behind the incident shock wave based on numerical calculations taking into account vibrational-chemical kinetics between the waves. Since there are no experimental data in this time range, the comparison is made with a similar prediction from [14] based on the QCT model. It is seen from all simulations that the mole fraction of atomic oxygen does not exceed 10^{-4}, which is negligible and, therefore, justifies the assumption about frozen chemical reactions between the waves made in [13, 15]. Comparing the evolution of χ_O with that from [14], one can see good agreement between the results obtained by two approaches, especially when $U = D/6k$ is used in our simulations.
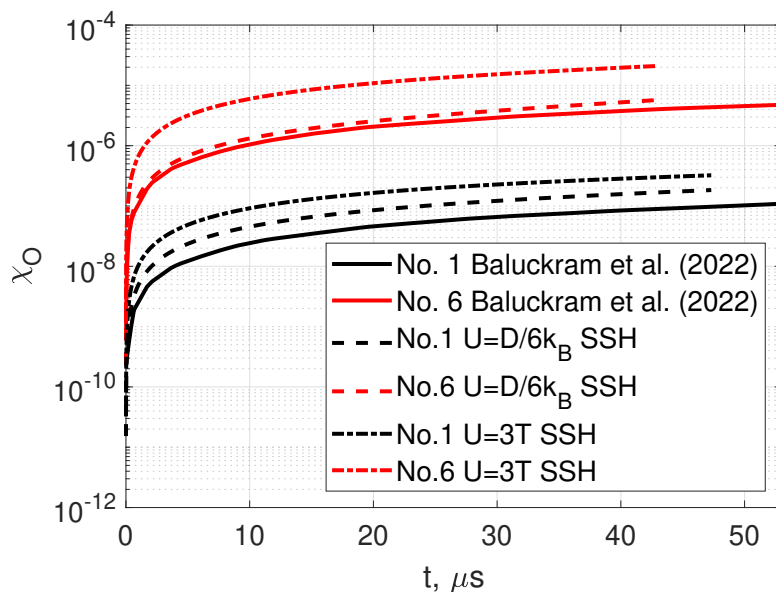

FIGURE 2. Atomic oxygen mole fraction predictions behind the incident shock waves in comparison with Baluckram et al.'s calculations [14].

Next, we assess the vibrational temperature time-histories. In addition to our previous study of vibrational temperature [15], here we improve the T_v definition and compare the results with recent QCT-based simulations of [14]. Usually the vibrational temperature in the state-to-state approach is calculated by the formula $T_v^{01} = \varepsilon_1 / (k \ln(n_0/n_1))$ (this is also used in [15]), where ε_1 is the vibrational energy of the first vibrational level. However, the authors of the experiment [13] extracted the vibrational temperature from the absorption data corresponding to the 5th and 6th vibrational levels due to the fact that at low vibrational states the distribution is close to the Boltzmann. Following that assumption, we added to the consideration the vibrational temperature calculated from the ratio of the populations of the 5th and 6th vibrational levels $T_v^{56} = (\varepsilon_6 - \varepsilon_5)/(k \ln(n_5/n_6))$. Figure 3 shows the time dependence of the vibrational temperature T_v^{56} in comparison with the experimental data and recent simulation results [14] for the
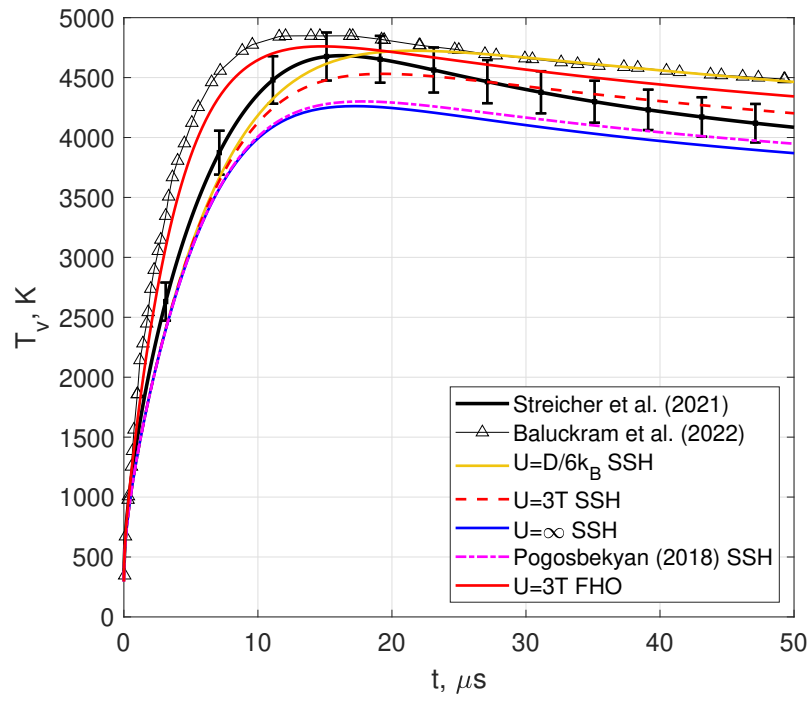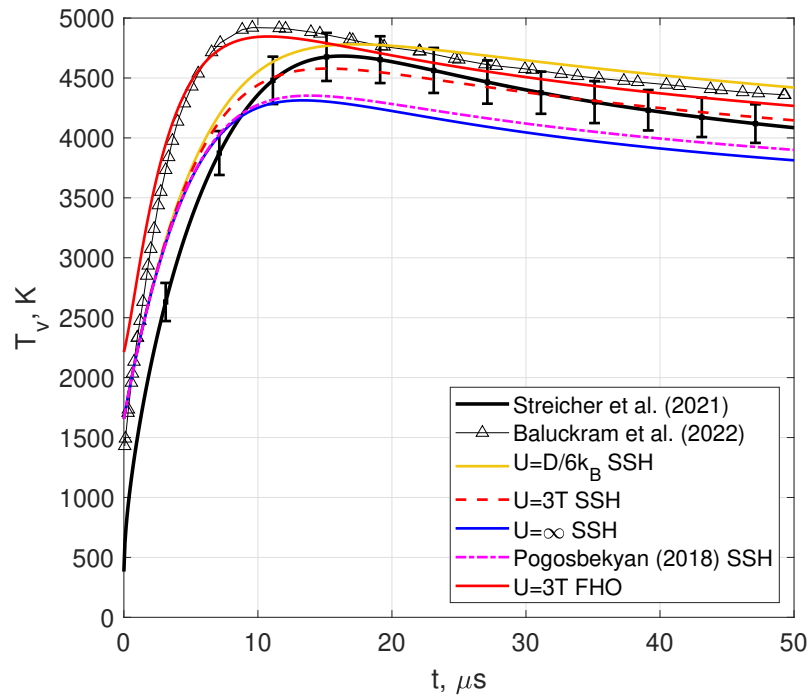
FIGURE 3. Vibrational temperature T_v^{56} time-histories behind the front of the reflected shock wave for initial conditions no. 1 without taking into account relaxation after the incident shock wave (a) and with taking relaxation into account (b).
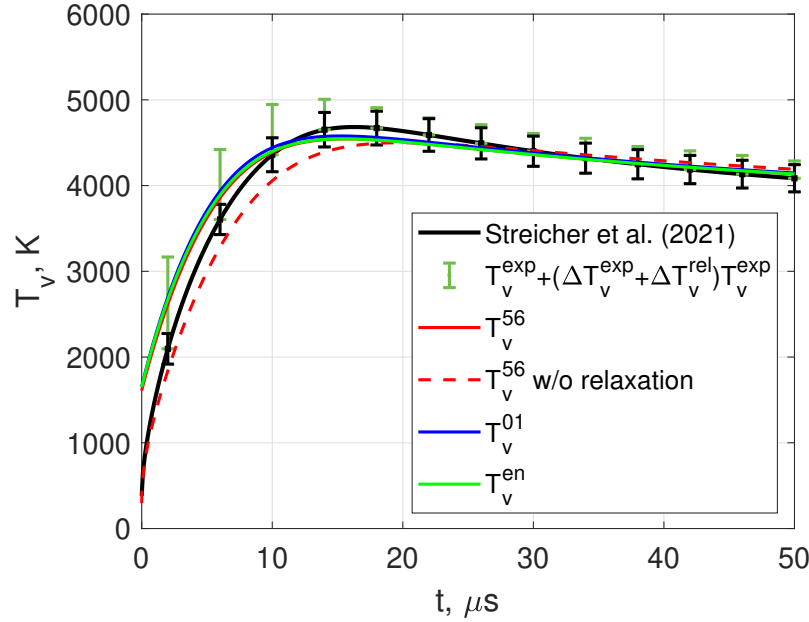
FIGURE 4. Comparison between T_v^{01}, T_v^{56} and T_v^{en} under conditions no. 1 taking into account relaxation after the incident shock wave. SSH vibrational energy exchange model and MT dissociation model with parameter $U = 3T$ are used. The usage of ΔT_v^{rel} is illustrated for the evaluation of the problem solution with partial relaxation.

cases with and without taking into account partial relaxation behind the incident SW. The temperature distributions are very similar to our previous results [15]. The SSH model generally describes the relaxation process well. As for the dissociation model, in all cases, the best agreement with the experiment is provided by the MT model with the parameter $U = 3T$. We note that the results obtained for the case without taking into account partial relaxation before the reflected SW are in better agreement with the data [13] for the vibrational temperature. In the case with taking into account relaxation between waves, we obtain a discrepancy in the initial values of the vibrational temperature, but both the magnitude and position of the T_v maximum are well described. However, this does not mean that partial relaxation should be neglected; it just shows that under the same initial conditions, we can obtain good agreement with [13]. More reliable comparison may be carried out for the absorbance time-histories; however at the moment we have no all necessary data for such an assessment.

The influence of partial relaxation between SWs was also evaluated in [14]. The vibrational temperature obtained taking into account relaxation also significantly differs from the experimental, especially at the initial moments behind the reflected SW. This once again indicates the presence of initial non-equilibrium and the importance of partial relaxation behind the incident SW. The initial T_v values in our simulations and in [14] differ, but only by 180 K, which is much less compared to the discrepancy with the experiment. Also interesting to note that the FHO model provides very similar with [14] results for both cases with and without relaxation between SWs. Although the FHO model was previously recommended in [10] based on the analysis of incident shock experiments [11], in the present case, it still overestimates T_v. Therefore, the use of a more advanced FHO-FR model is of particular interest. Moreover, we are going to compare absorbance time-histories, which may lead to results reassessment. It is worth recalling that the partial relaxation time between passing of two waves was estimated to be comparable with the experimental measurement time [15].

Figure 4 presents assessment of different approaches to the calculation of vibrational temperature. The comparison was made for the test case corresponding to the experimental conditions no. 1 taking into account the relaxation between waves. The difference between T_v^{01} and T_v^{56} is found negligible due to the near-Boltzmann distribution. We also considered the vibrational temperature calculated from the total vibrational energy. To find T_v^{en}, the following

nonlinear equation was solved

$$E_{\text{vibr}} = \sum_{i=0}^{l} n_i(\varepsilon_i + \varepsilon_0) = \frac{n_m}{Z_{\text{vibr}}} \sum_{i=0}^{l} \exp\left(-\frac{\varepsilon_i}{kT_v^{\text{en}}}\right)(\varepsilon_i + \varepsilon_0), \quad \text{where } n_m = \sum_{i=0}^{l} n_i, \quad Z_{\text{vibr}} = \sum_{i=0}^{l} \exp\left(-\frac{\varepsilon_i}{kT_v^{\text{en}}}\right).$$

In the above expression, the time-dependent vibrational distributions n_i are obtained from non-equilibrium flow modeling. Figure 4 also demonstrates the negligible difference between T_v^{en} and T_v^{56}. Such behaviour justifies the assumption of the Boltzmann distribution on the low vibrational states. In reality, immediately behind the SW front the distribution is strongly non-equilibrium with the unpopulated tail on high energy states; however, these states weakly contribute to the total vibrational energy. The previous T_v analysis in Figure 3 is carried out using T_v^{56} due to its better connection to the experimental results [13]. However, this does not change the general qualitative picture compared to our previous study [15].

To evaluate the difference in vibrational temperatures obtained with and without relaxation, we propose the following estimate

$$\Delta T_v^{\text{rel}} = \frac{T_v^{\text{rel}} - T_v^{\text{fr}}}{T_v^{\text{fr}}},$$

where T_v^{rel} is the simulated vibrational temperature accounting for the partial relaxation and T_v^{fr} is that with frozen processes between SWs. To be able to compare complete setting simulations with the experiment [13] we suggest to use ΔT_v^{rel} as an additional approximate correction to the experimental error. Figure 4 illustrates it. The value of the vibrational temperature, certainly, should depend on the chosen dissociation model, however, the dependence of ΔT_v^{rel} on the dissociation model is found very weak. It allows us to construct this correction. For our calculations the max ΔT_v^{rel} value was obtained at $t = 0$ μs and is equal 444%. At the T_v maximum it decreases to about 2% and becomes almost zero at $t = 50$ μs. To better evaluate the correction Δ, an accurate technique of extracting T_v from experimental absorbance is required.

CONCLUSION

State-to-state simulations of pure oxygen flows under post-reflected shock conditions are carried out in order to extend our recent study [15] and complement it with new comparisons and clarifications. Two vibrational energy exchange models and four values of nonequilibrium parameter U in the state-specific Marrone–Treanor dissociation model are used. Simulations are done taking into account and neglecting vibrational and chemical relaxation between incident and reflected shock waves. Pressure, atomic mole fraction and vibrational temperature time-histories are compared with experimental data [13] and theoretical QCT-based numerical study [14]. It is shown that neglecting chemical reactions behind an incident SW does not alter the flow whereas excluding partial vibrational relaxation causes significant pressure underestimation. Simulations of the reflected shock wave propagating through the relaxing gas show good agreement of the pressure evolution with experimentally measured pressure time-histories.

The question about vibrational relaxation between the incident and reflected waves is particularly important for the vibrational temperature evaluation. We got further confirmation of the results published earlier in [14, 15]. When partial relaxation is taken into account, the initial values of simulated T_v behind the front of the reflected SW are larger than the experimental data, however, they are in good agreement with the results obtained in [14]. The reason for the discrepancy is in the assumption of frozen vibrational kinetics used by the experimenters for extracting T_v from the data on absorbance. This once again indicates the importance of taking partial relaxation into account in the postprocessing of experimental data.

We also compared different ways to define the vibrational temperature and showed their equivalence. The vibrational temperature was modeled based on the populations of the 5th and 6th vibrational levels, just as in the experiment [13]. It was shown that the vibrational temperature calculated in this way differs very weakly from the vibrational temperature calculated relative to the 1st and 0th vibrational levels. For all cases, the best agreement with the experiment was obtained using the combination of the SSH and MT models with $U = 3T$. Surprisingly, the FHO model gives close agreement with QCT-based simulations [14] but not with experimental data.

For more accurate comparison with experimental data we propose an additional correction to the experimental error which takes into account the effect of vibrational relaxation between the incident and reflected shock. This correction is large near the shock front but tends to zero with rising time. In the future work, we plan to simulate the oxygen absorbance directly and compare it with the experimental measurements, thus avoiding uncertainties introduced by experimental data postprocessing.

ACKNOWLEDGMENTS

REFERENCES

1. G. A. Bird, *Molecular Gas Dynamics and the Direct Simulation of Gas Flows* (Clarendon, Oxford, England, UK, 1994).
2. S. F. Gimelshein, J. Thermophys. Heat Transf. **35**, 362–371 (2021).
3. E. Nagnibeda and E. Kustova, *Nonequilibrium Reacting Gas Flows. Kinetic Theory of Transport and Relaxation Processes* (Springer Verlag, Berlin, Heidelberg, 2009).
4. S. F. Gimelshein, I. J. Wysong, A. J. Fangman, D. A. Andrienko, O. V. Kunova, E. V. Kustova, C. Garbacz, M. Fossati, and K. Hanquist, J. Thermophys. Heat Transf. **36**, 399–418 (2022).
5. S. F. Gimelshein, I. J. Wysong, A. J. Fangman, D. A. Andrienko, O. V. Kunova, E. V. Kustova, F. Morgado, C. Garbacz, M. Fossati, and K. M. Hanquist, J. Thermophys. Heat Transf. **36**, 870–893 (2022).
6. O. Kunova, E. Kustova, M. Mekhonoshina, and E. Nagnibeda, Chem. Phys. **463**, 70–81 (2015).
7. O. V. Kunova, E. V. Kustova, M. Yu. Melnik, and A. S. Savelev, Phys. Chem. Kinetics Gas Dynam. **19** (2018), (in Russian).
8. I. Kadochnikov and I. Arsentiev, Journal of Physics D: Applied Physics **51**, 374001 (2018).
9. H. Luo, I. B. Sebastião, A. A. Alexeenko, and S. O. Macheret, Phys. Rev. Fluids **3**, 113401 (2018).
10. L. Campoli, O. Kunova, E. Kustova, and M. Melnik, Acta Astronaut. **175**, 493–509 (2020).
11. L. B. Ibraguimova, A. L. Sergievskaya, V. Y. Levashov, O. P. Shatalov, Y. V. Tunik, and I. E. Zabelinskii, J. Chem. Phys. **139**, 034317 (2013).
12. I. J. Wysong, S. F. Gimelshein, N. E. Bykova, O. P. Shatalov, and I. E. Zabelinski, AIP Conference Proceedings **2132**, 180008 (2019).
13. J. W. Streicher, A. Krish, and R. K. Hanson, Phys. Fluids. **33**, 056107 (2021).
14. V. T. Baluckram, A. J. Fangman, and D. A. Andrienko, J. Thermophys. Heat Transf. **37**, 198–212 (2022).
15. D. S. Kravchenko, E. V. Kustova, and M. Y. Melnik, Vestn. St. Petersbg. Univ.: Math. **55**, 281–289 (2022).
16. R. N. Schwartz, Z. I. Slawsky, and K. F. Herzfeld, J. Chem. Phys. **20**, 1591–1599 (1952).
17. I. V. Adamovich, S. O. Macheret, J. W. Rich, and C. E. Treanor, J. Thermophys. Heat Transf. **12**, 57–65 (1998).
18. P. V. Marrone and C. E. Treanor, Phys. Fluids **6**, 1215–1221 (1963).
19. C. Park, J. T. Howe, R. L. Howe, R. L. Jaffe, and G. V. Candler, J. Thermophys. Heat Transf. **8**, 9–23 (1994).
20. M. Yu. Pogosbekyan and A. L. Sergievskaya, Russian Journ. Phys. Chem. B **12**, 208–218 (2018).
21. I. V. Adamovich and J. W. Rich, J. Chem. Phys. **109**, 7711–7724 (1998).
22. I. V. Adamovich, AIAA J. **39**, 1916–1925 (2001).